Available online at www.sciencedirect.com
ScienceDirect
Fuel 87 (2008) 885–893
FUEL
www.fuelfirst.com

Transformation of alkali and alkaline earth metals in low rank coal during gasification

Koichi Matsuoka [a,*], Toru Yamashita [b], Koji Kuramoto [a], Yoshizo Suzuki [a], Akira Takaya [c], Akira Tomita [c]

[a] National Institute of Advanced Industrial Science and Technology (AIST), 16-1 Onogawa, Tsukuba 305-8569, Japan
[b] Idemitsu Kosan Co. Ltd., 3-1 Nakasode, Sodegaura 299-0267, Japan
[c] Institute of Multidisciplinary Research for Advanced Materials, Tohoku University, 2-1-1 Katahira, Aoba-ku, Sendai 980-8577, Japan

Received 16 November 2006; received in revised form 26 March 2007; accepted 3 May 2007
Available online 12 June 2007

Abstract

Transformation of alkali and alkaline earth metals (AAEM) in low rank coals during gasification was examined by combining computer-controlled scanning electron microscopy (CCSEM) and inductively coupled plasma-atomic emission spectroscopy (ICP-AES). Two sub-bituminous coals were pyrolyzed at 1500 °C using a drop tube furnace, and the resultant chars were then gasified in CO_2 atmosphere at the same temperature. Total amounts of AAEM species in the raw coals and the chars were determined by ICP-AES. Minerals in the raw coals and ash particles in the chars were analyzed by CCSEM.

AAEM species were mainly present in the raw coals as dispersed species, organically associated cations or fine mineral particles (<1 μm), which cannot be quantified by CCSEM. It was found that the dispersed Ca species were first converted into fine ash particles upon the devolatilization and then most of the particles interacted with inherent clay minerals to form complex aluminosilicates. In the case of Na and K, the dispersed species mostly vaporized and the interaction with inherent minerals was not observed.

Keywords: Computer-controlled scanning electron microscope; Ash; Alkali and alkaline earth metal

1. Introduction

Alkali and alkaline earth metals (AAEM) in low rank coals mainly exist as organically associated cations or in discrete minerals. In coal conversion processes, organically associated AAEM cations play an important role. Many studies have been done to clarify the role of cations on pyrolysis [1–4], gasification [5–7], combustion [8–16], and liquefaction [17]. For example, it is well known that organically associated AAEM cations of low rank coals act as a catalyst in steam gasification [5–7]. On the other hand, AAEM species bring about an undesirable effect in some cases. Interaction of AAEM with discrete minerals may reduce the melting point of mineral particles, and the resultant ash contributes easily to coalescence or agglomeration [13,14]. This causes some problem, for example, agglomeration of bed materials in fluidized bed combustion. Therefore, it is important to understand the fate of AAEM species.

To understand the ash formation during the combustion of low rank coals, many researchers have compared the information obtained by computer-controlled scanning electron microscopy (CCSEM) about the composition of inorganics in the raw coal and in the fly ash [9–15]. These studies mainly focused on the ash formation behavior during combustion, and little attention was paid to ash formation during gasification. In our previous study, ash particles in the gasified Beulah Zap lignite char were analyzed by CCSEM [18], and the fate of Na and Ca in the initial stage of the lignite gasification has been clarified.

* Corresponding author. Fax: +81 29 861 8209.
E-mail address: koichi-matsuoka@aist.go.jp (K. Matsuoka).

0016-2361/$ - see front matter © 2007 Elsevier Ltd. All rights reserved.
doi:10.1016/j.fuel.2007.05.031

However, quantitative analysis such as partitioning of the AAEM species to gas phase and to ash and the ash formation mechanism at a high conversion stage was not examined. Therefore, this study is an attempt to quantitatively clarify the fate of AAEM species of two low rank coals during pyrolysis and the subsequent gasification. The ash particles in the pyrolyzed chars and the gasified chars were analyzed mainly by CCSEM. CCSEM method has an inherent limitation; it cannot quantify dispersed inorganic species [18]. Dispersed inorganic species denotes, in this paper, not only ion-exchanged metal ions but also fine mineral particles with a size of less than 1 μm. To overcome this weak point, an inductively coupled plasma-atomic emission spectrometric (ICP-AES) method was used to quantitatively determine the total amount of metal species in the samples.

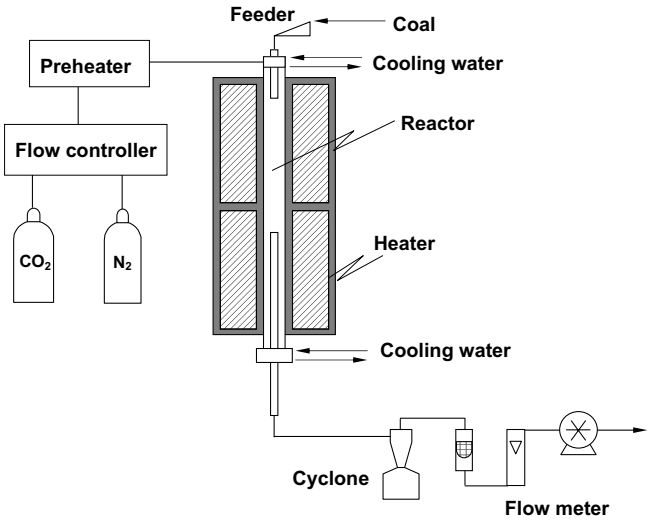

Fig. 1. Schematic diagram of a drop tube furnace.

2. Experimental

Two sub-bituminous coals (SS012 and SS070) supplied from Japan Coal Energy Center were used in this study. The analyses of the coals are presented in Table 1. The coal particles with a size from 45 to 75 μm were pyrolyzed under N_2 atmosphere at 1500 °C in a drop tube furnace as shown in Fig. 1. Particle heating rate was estimated as 10^3 K/s, and the particle residence time was estimated as 1.2 s. In gasification experiments, a once-pyrolyzed char was dropped into the reactor under the atmosphere of 100% CO_2 at 1500 °C. The extent of gasification was changed by changing the residence time. Detailed procedure of char preparation has been described elsewhere [19]. The amounts of the AAEM species were determined as follows. The raw coal or the char was subjected to ashing in a low-temperature oxygen plasma asher and then fused with a flux ($Li_2B_4O_7$) at 900 °C, followed by dissolution in aqueous HNO_3. Thereafter the solution was analyzed by ICP-AES (Horiba Ultima2). Minerals in the raw coal and ash particles in the char were analyzed by CCSEM (Hitachi S350-N/EDAX Genesis). The composition of more than thousand particles was determined and then categorized each ash particle as single element, two elements, three elements, four elements, and "others" using the category proposed by Chen et al. [8]. Single element category corresponds to the particles in which one element is >80% and the contents of all other elements are <10%. Two elements category includes those that contain more than 80% of any two elements with no third elements of >10%. Particles assigned to three elements (four elements) category contain >80% of any three (four) elements with no fourth (fifth) elements of >10%. Particles not meeting any of these criteria are placed in "others" category. Details of the CCSEM analytical procedure have been described elsewhere [18].

Table 1
Chemical analysis of the coals used in this study

	Proximate analysis (wt%, dry)			Ultimate analysis (wt%, daf)				
	Ash	VM	FC	C	H	N	S	O
SS012	2.8	46.4	50.8	72.3	5.2	1.4	0.4	20.8
SS070	6.1	54.8	56.6	74.5	5.3	1.4	0.1	18.7

Ash composition (wt% of ash, sulfur-free basis)

	SiO_2	Al_2O_3	Fe_2O_3	CaO	K_2O	MgO	TiO_2	Na_2O	P_2O_5
SS012	35.7	23.4	14.7	14.7	0.9	5.3	1.3	1.1	3.0
SS070	47.4	20.1	10.0	13.8	0.8	3.9	1.1	2.3	0.5

3. Results

3.1. Contents of AAEM in raw coal and char

Inorganics in low rank coal can be classified into mineral form and non-mineral form (ions dissolved in the pore waters and the organically associated cation). Chemical fractionation method, that is, successive leaching with water, ammonium acetate, and HCl, is widely used to quantify ions dissolved in the pore waters, the organically associated cation and mineral, respectively [20,21]. In this study, for the simplification, inorganics are classified into two fraction; mineral and non-mineral. Then the fate of AAEM species of two low rank coals during gasification is clarified. Some researchers reported that mineral and non-mineral can be classified by leaching with ammonium acetate [20,21]. However, in our previous study it was found that not only non-mineral Ca but also a part of Ca-containing mineral such as $CaCO_3$ was removed by leaching with ammonium acetate [22]. If one considers the leached Ca being equal to non-mineral Ca, the leaching method leads to overestimation of the amount of non-mineral Ca. Ions dissolved in the pore waters, organically associated cations, and fine minerals below 1 μm cannot be quantified by CCSEM, but discrete minerals with a size of more than 1 μm can be quantified. Thus the unquantifi-

able species was determined as the difference between the total amount of each element determined by ICP-AES and the amount quantified by CCSEM. In the preliminary experiment, the amount of Ca leached out with ammonium acetate in SS012 coal was determined and its amount was larger than that of dispersed Ca species (Fig. 2). Dissolution of a part of Ca minerals during leaching could also be confirmed from the preliminary experiment. Hence, the leaching method was not applied further to determine the mode of occurrence in this study. As stated before, the unquantifiable fraction (organically associated cations, ions, and fine minerals below 1 μm) is termed as "dispersed species" in this study, and the fate of the dispersed species during gasification is examined.

Fig. 2 shows weight fraction of the CCSEM-quantifiable AAEM species and the unquantifiable species in the raw coals. The AAEM species in the two coals are mainly present as dispersed species. For example, about half of Ca-containing species are present as dispersed species in the SS012 coal, while almost all Mg species in the same coal are dispersed species. The mode of occurrence of each metal is not the same between two coals, but the fraction of dispersed species is more or less similar.

In Fig. 3, the total amounts of the AAEM in the raw coal and the resultant char determined by ICP-AES were plotted against the carbon conversion, X_C, which is defined on the basis of the initial carbon weight in the parent coal. The content in the raw coal is plotted at $X_C = 0$, and that in the pyrolyzed coal around $X_C = 50$. The trend of retention behavior was dependent on the type of metal. Almost all Ca and Mg were retained in the gasified char even at an X_C of 80%. About half of Na vaporized upon pyrolysis, and further vaporization occurred during the gasification for both the coals. The behavior of K is somewhat different for the two coals. The loss of K was hardly observed in SS012 coal both during pyrolysis and gasification. However, in the case of SS070 coal, vaporization of K was observed in both the stages.

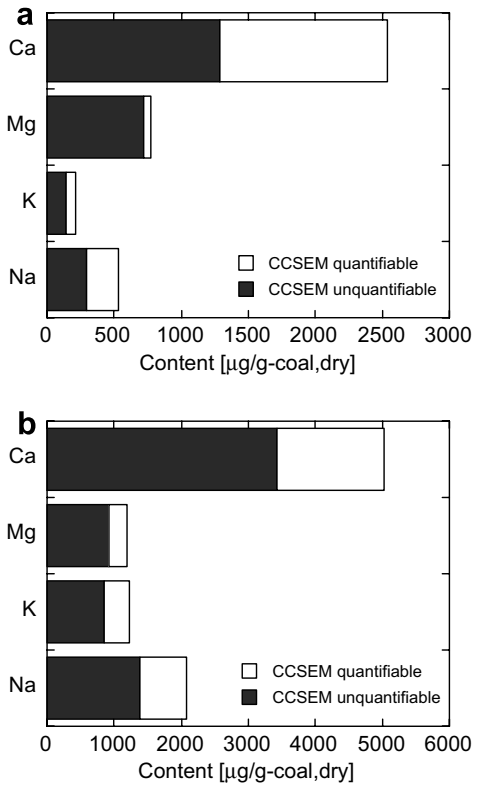

Fig. 2. Mode of occurrence of AAEM in coal: (a) SS012 coal and (b) SS070 coal.

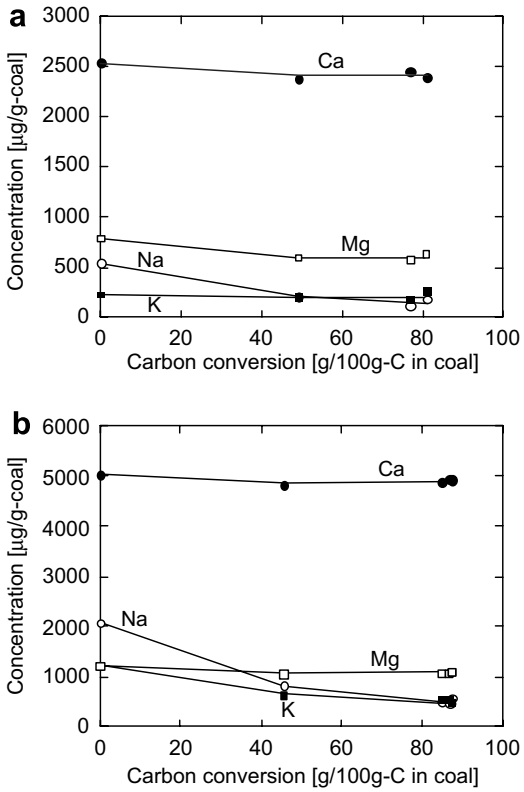

Fig. 3. Relationship between total AAEM contents as determined by ICP-AES and carbon conversion during pyrolysis and gasification: (a) SS012 coal and (b) SS070 coal.

3.2. CCSEM analysis of minerals in raw coals and ash in chars

Inorganic constituents in the raw coal and the chars were analyzed by CCSEM. The inorganic constituents in the pyrolyzed char are called here as "ash" as a matter of convenience. Fig. 4 represents back-scattered electron (BSE) images of the SS070 raw coal, pyrolyzed char, and gasified char. Bright particles in Fig. 4a were the mineral particles and those in Fig. 4b and c were the ash particles. In the back-scattered electron images, ash particles in the pyrolyzed char were not so clearly visible, while a number of spherical ash particles were observed on the surface of the gasified char. The trend was similar in both coals. This morphology evidently suggests melting of ash particles during the gasification, probably due to the interaction of

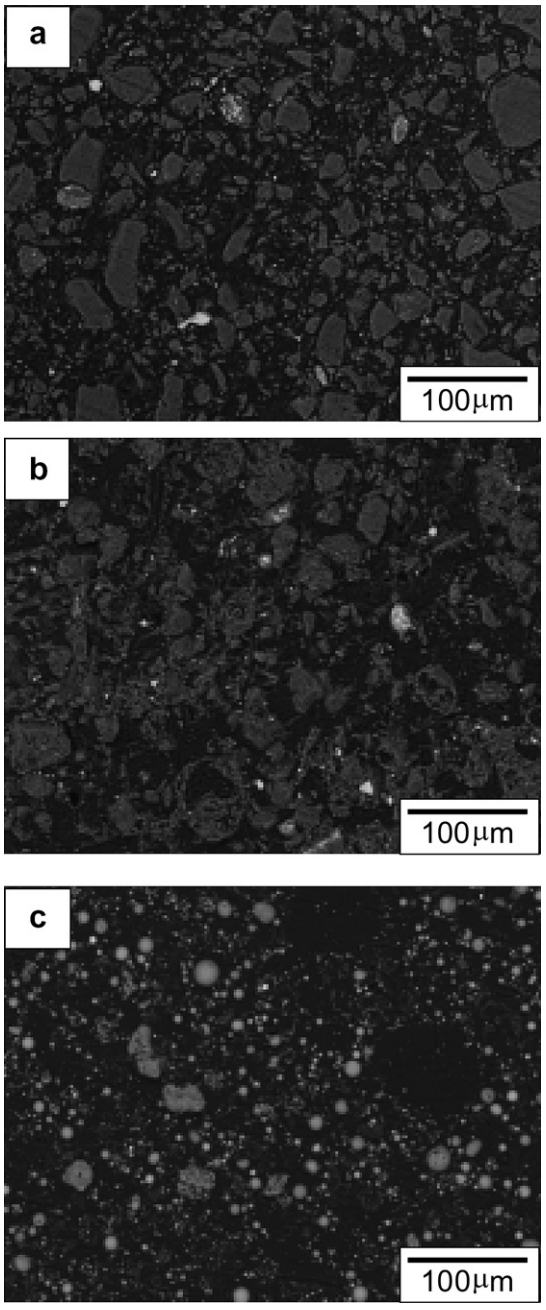

Fig. 4. Back-scattered images of (a) SS070 raw coal, (b) pyrolyzed char, and (c) gasified char ($X_C = 88\%$).

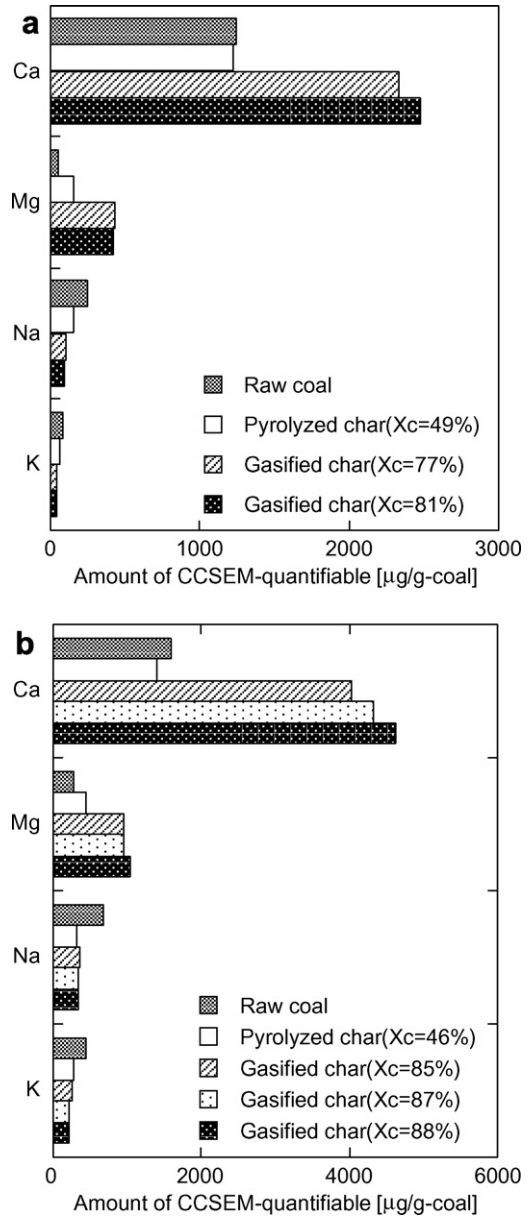

Fig. 5. CCSEM-quantifiable amounts of AAEM in the raw coal and the char: (a) SS012 coal and (b) SS070 coal.

AAEM species retained in the pyrolyzed char (Fig. 3) with the inherent minerals to form ash particles with low-melting points.

Fig. 5 shows the AAEM content in the raw coals and the resultant chars as determined by CCSEM. The content is represented on the basis of unit weight of the parent coal. The amounts of CCSEM-quantifiable Ca and Mg did not change upon pyrolysis but they apparently increased after the gasification. The increase of Ca and Mg content suggests that the dispersed Ca and Mg species not quantified by CCSEM, were converted to CCSEM-quantifiable species during the gasification. On the other hand, the CCSEM-quantifiable amounts of Na and K slightly decreased upon gasification. This indicates that the transformation of dispersed Na and K species into CCSEM-quantifiable ash particles was not remarkable, while the loss of Na- and K-containing inherent minerals due to vaporization took place to some extent.

Fig. 6 shows the weight fraction of CCSEM-quantifiable minerals in the raw coals as well as weight fraction of CCSEM-quantifiable ash species in the chars. Dominant minerals in the SS012 coals were Si (quartz), Si–Al (kaolinite), Fe–S (pyrite), and Ca–Al–P (crandallite). No significant change was seen for Si and Si–Al upon pyrolysis, and little increase was seen for aluminosilicates such as Ca–Al–Si. The contents of Si and Si–Al were decreased upon the gasification, while Ca–Al–Si, Fe–Al–Si, and Ca–Fe–Al–Si

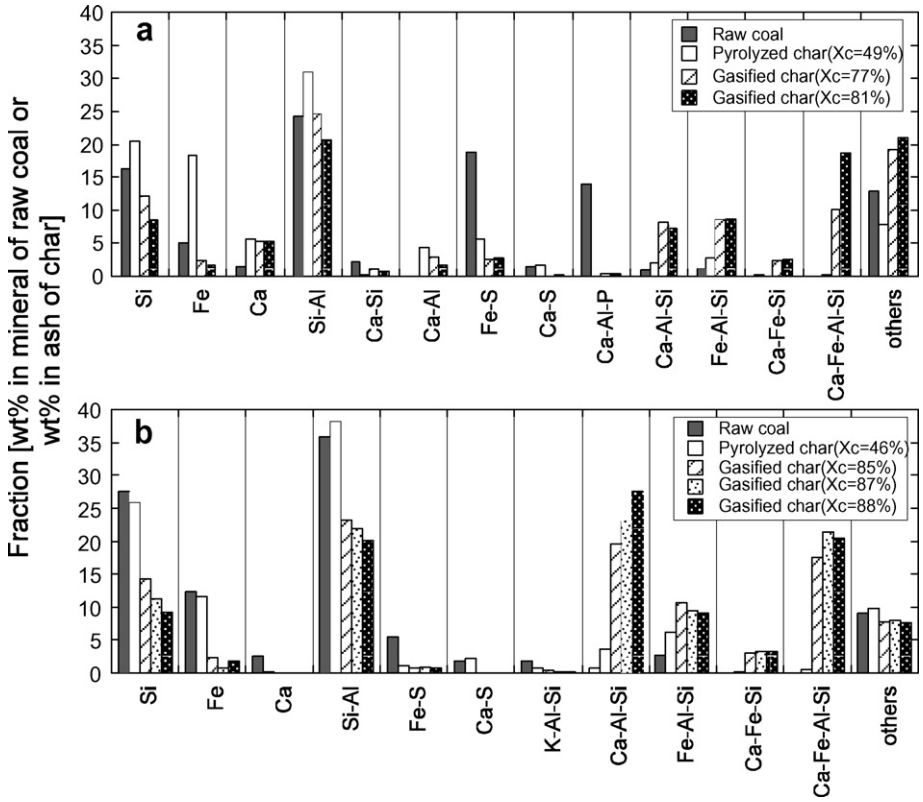

Fig. 6. Weight fraction of mineral species in the raw coal and weight fraction of ash species in the char: (a) SS012 coal and (b) SS070 coal.

were increased. Fe–S decreased drastically on pyrolysis, while Fe (presumably iron oxide) increased to a large extent upon pyrolysis and then decreased during the gasification. Similar trends for Si, Si–Al, Ca–Al–Si, Fe–Al–Si, and Ca–Fe–Al–Si were observed in the case of SS070 coal. Interaction of AAEM species with inherent quartz and clay minerals was not seen during pyrolysis at 1500 °C but commenced on the gasification.

The dependence of the content of Ca and Na species retained in the char on carbon conversion, X_C, is shown in Fig. 7. Though not shown here, the trend of Mg was similar to that of Ca. The dispersed Ca was still unquantifiable by CCSEM after pyrolysis. Conversion of dispersed Ca to CCSEM-quantifiable species became apparent at high conversion stage. In the case of Na, the amount of CCSEM-quantifiable fraction decreased on pyrolysis and CCSEM-quantifiable Na species mainly unchanged after gasification.

3.3. Ca-containing ash in char

Ca is the most abundant element among AAEM and it significantly contributes to the formation of low-melting point ash. Therefore, the behavior of Ca-containing ash was examined in detail. Composition of ash particles that contain Ca + Al + Si > 80% is plotted in a ternary diagram (Fig. 8). In the case of SS012 pyrolyzed char (Fig. 8a), most of the particles are distributed either on the Si–Al join, the Ca rich apex, or the Ca–Al join. The ternary diagram for the SS012 gasified char (Fig. 8b) indicates the presence of particles with compositions ranging from the Ca rich apex towards the midpoint of the Si–Al join. In the case of the pyrolyzed SS070 char (Fig. 8c), most of the particles were distributed along the Si–Al join. In the gasified char (Fig. 8d), in addition to these particles, many particles having a composition corresponding to the Ca–Al–Si center were detected.

Fig. 9 shows the Ca content in each inorganic species in the raw coal, the pyrolyzed char, and the gasified char. The total amount of Ca was determined by ICP-AES. The Ca-containing minerals in the raw coal and Ca-containing ash in the char were quantified by CCSEM. The difference between the total amount and the CCSEM-quantifiable fraction is the CCSEM-unquantifiable fraction (shown as "dispersed Ca < 1 μm"). Sum of the CCSEM-quantifiable fraction in SS012 raw coal was similar to that of the pyrolyzed char as shown in the upper part of Fig. 9a. Big differences between the raw coal and the pyrolyzed char are (a) increase of "Ca" (presumably CaO), (b) appearance of "Ca–Al" and "Ca–Al–Si", and (c) disappearance of "other ash" and "Ca–Al–P" (mainly crandallite). The amount of "Ca" did not change much before and after gasification. The "dispersed Ca" in the pyrolyzed char disappeared during the gasification, while "Ca–Al–Si", "Ca–Fe–Al–Si", and "other ash" remarkably increased during the gasification. Although the conversion (X_C) was not so varied, the

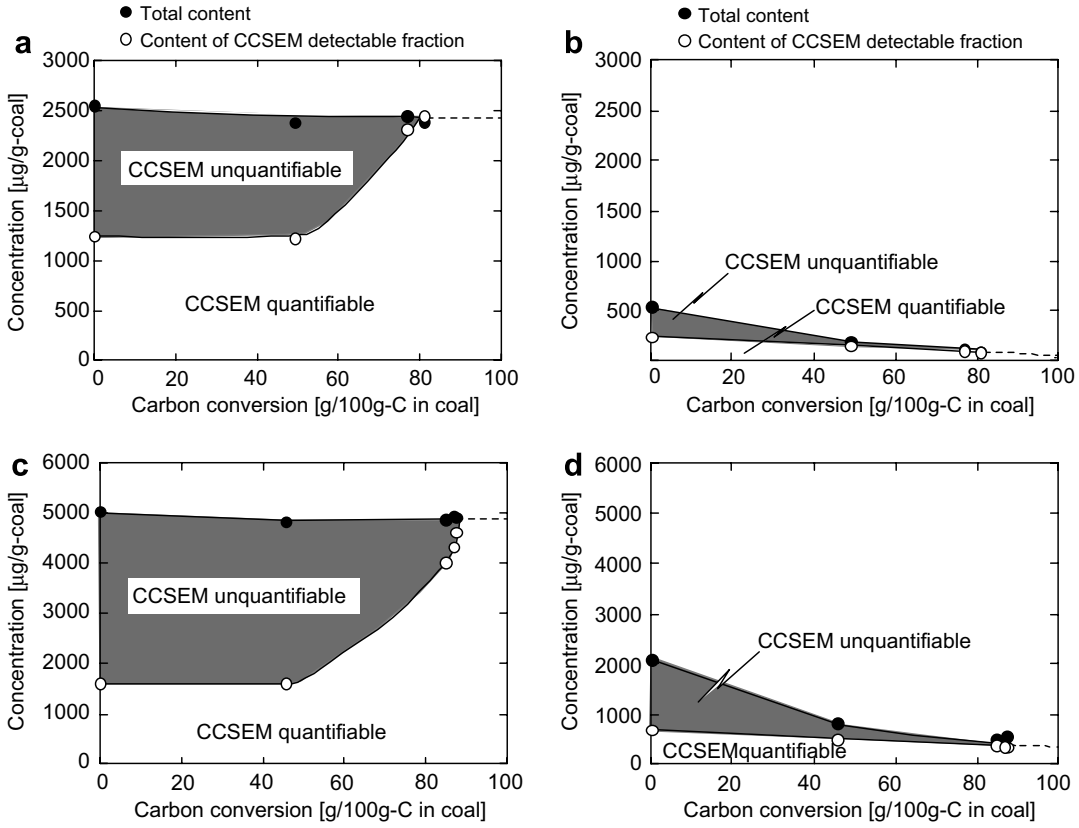

Fig. 7. Change of mode occurrence of Ca and Na with carbon conversion during pyrolysis and gasification: (a) Ca in SS012 coal, (b) Na in SS012 coal, (c) Ca in SS070 coal, and (d) Na in SS070 coal.

amount of "Ca–Fe–Al–Si" is likely to increase with increasing X_C. Interaction of Ca species with clay minerals in the char matrix increased due to the disappearance of the char matrix at a high conversion stage.

Contrary to SS012, little "Ca" was present in SS070 pyrolyzed char as well as in gasified char. Some increase of "CaS", "Ca–Al–Si", and "other ash" was observed after pyrolysis, and "Ca–Al–Si", "Ca–Fe–Al–Si", and "other ash" were found to be the main species in the gasified char.

4. Discussion

4.1. Fate of Na and K during gasification

It is well known that aluminosilicates behave as accepter of Na and K species during combustion, and Na– and K–aluminosilicates are dominant species in the ash [26]. Noda et al. examined vaporization of Na- and K-including minerals during combustion and gasification [16]. They reported that vaporization of Na and K were more significant in the case of gasification than combustion because CO formed during the gasification promoted the decomposition of minerals and then resulted in vaporization of metallic Na and K. The decrease of CCSEM-quantifiable Na and K during the gasification in Fig. 5 may also be enhanced by the presence of CO formed during the gasification stage. Furthermore, even if Na- and K-aluminosilicates are formed under the present gasification conditions, these amounts were very small as is seen in Fig. 6. It means that vaporization of dispersed Na and K species are a predominant pathway during the gasification rather than the formation of Na- and K-containing aluminosilicates.

4.2. Fate of Ca during pyrolysis

Extent of Ca loss during pyrolysis will be discussed first. Fig. 9 clearly indicates that there was little vaporization loss in total Ca content for both coals. This is in apparent contrast with the results reported by Li et al. [2], where they observed about 40% loss of Ca during the pyrolysis of Ca-exchange Loy Yang coal at 1200 °C in a wire-mesh reactor. This discrepancy is likely due to the difference in the sample itself and/or experimental technique. They prepared their sample by removing organically associated cation by rigorous acid washing and introducing Ca by ion-exchange method and hinted that this procedure may have modified the structure of coal. Thus the behavior of introduced Ca ion may be different from inherently associated Ca. Manzoori and Agarwal carried out pyrolysis experiment with a fluidized bed reactor at 700–830 °C using a non-treated Australian brown coal [24]. The result was similar to our present result; they observed almost no vaporization loss of Ca.

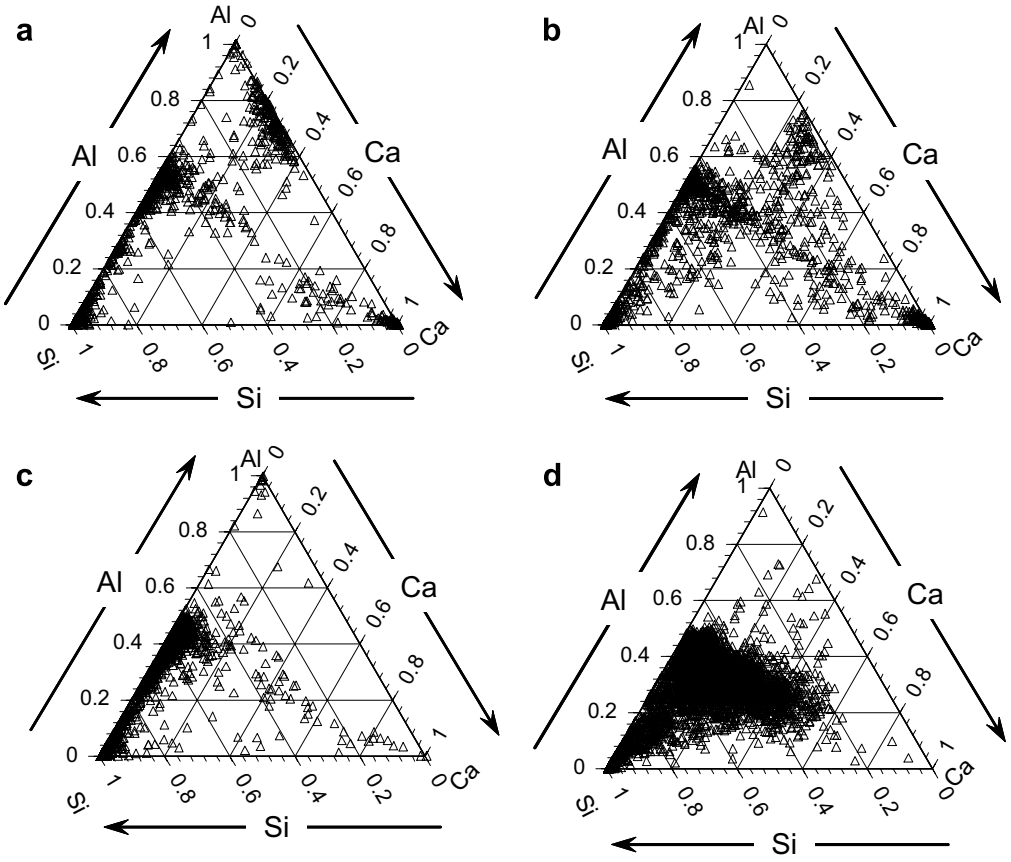

Fig. 8. Ternary diagrams for ash particles containing >80% of Ca + Si + Al: (a) SS012 pyrolyzed char, (b) SS012 gasified char ($X_C = 81\%$), (c) SS070 pyrolyzed char, and (d) SS070 gasified char ($X_C = 88\%$).

The change of Ca-containing minerals during pyrolysis is an interesting topic for discussion. Fig. 9 shows remarkable difference between SS012 and SS070 coals with respect to the change of discrete mineral matter upon pyrolysis. Major change in SS012 was a complete disappearance of "Ca–Al–P (mostly crandallite)" and "other ash", leading to a large increase of "Ca" and a small increase of "Ca–Al" and "Ca–Al–Si". Guardani et al. [28] examined a transformation of aluminum phosphate rocks including crandallite ($CaAl_3(PO_4)_2(OH)_5H_2O$) during calcination in a fluidized bed. According to their report, crandallite decomposes to calcium phosphate ($Ca_3(PO)_4$), phosphocristobalite ($AlPO_4$), and alumina (Al_2O_3) during calcination at 900–1100 °C. On the other hand, Iwabu et al. [29] examined the fate of calcium phosphate (product of calcination of aluminum phosphate) in sewage sludge melting process. When calcium phosphate ($Ca_3(PO)_4$) is treated with carbon and silica at around 1400 °C for 4 h, calcium phosphate transformed as follows:

$$2Ca_3(PO_4)_2 + 6SiO_2 + 10C = 6CaO + 2P_2O_5 + 6SiO_2 + 10C = 6CaSiO_3 + P_4 + 10CO$$

The pyrolysis condition in the present study is similar to that by Iwabu et al. [29]. Judging from the above studies [28,29], crandallite in SS012 coal might first decompose to $Ca_3(PO)_4$, $AlPO_4$, and Al_2O_3. Then $Ca_3(PO)_4$ further decomposed to CaO, but CaO did not interact with SiO_2 to form $CaSiO_3$, because the reaction time (1.2 s) was quite short. One can infer that the disappearance of "Ca–Al–P" upon pyrolysis was not due to its vaporization but due to the transformation to "Ca".

Contrary to SS012, "Ca" species in SS070 decreased upon pyrolysis, and some increase was observed for "CaS", "Ca–Al–Si", and "other ash". It is well known that "CaS" can be formed due to the interaction between CaO and S-containing gas evolved upon pyrolysis. Other details are not clear at the present moment.

The amount of finely dispersed minerals was not small; it was about a half of the total inorganics for SS012 coal and about two-thirds for SS070 char. Although the chemical species in "dispersed Ca" cannot be identified by the present CCSEM study, SEM/EDX mapping analysis combined with XRD analysis revealed that the dispersed Ca species in SS012 pyrolyzed char was submicron CaS particles [23]. The raw coal does not contain these species but "ion-exchanged Ca" and "Ca particles of a size <1 μm" were the main constituents. Therefore, it was concluded that such dispersed Ca species present in the raw coal were transformed to finely dispersed CaS species as a consequence of reaction with S-containing gas evolved during pyrolysis. The S/Ca atomic ratio in SS012 coal is 1.2, and

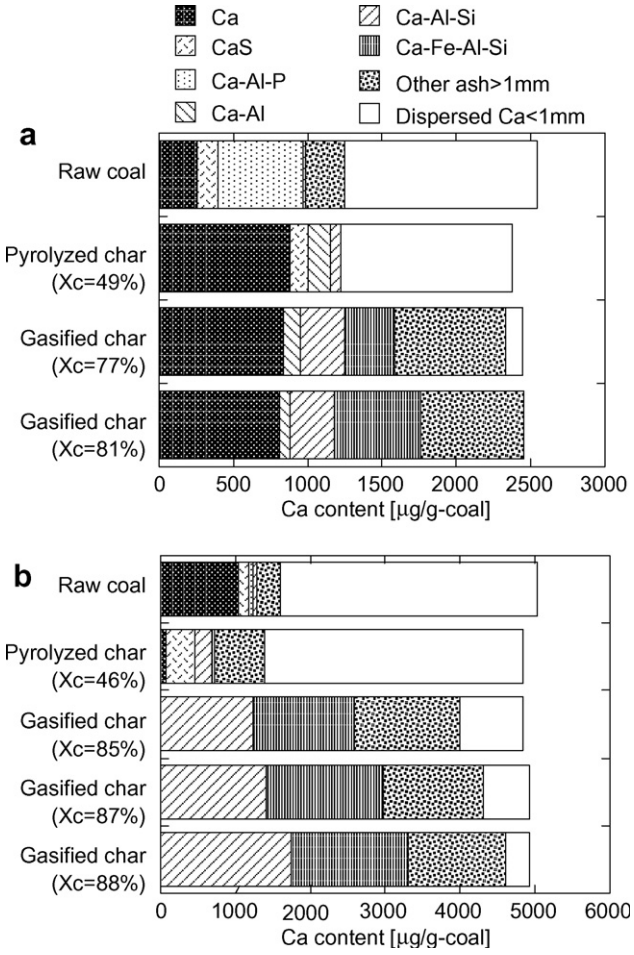

Fig. 9. Ca content in inorganic species in the raw coal, the pyrolyzed char, and the gasified char: (a) SS012 coal and (b) SS070 coal.

it is possible for most Ca ions to be converted to CaS. The pyrolysis behavior of SS070 coal is somewhat different from SS012 coal, but the amount of dispersed Ca before and after pyrolysis is almost the same as in the case of SS012. From the present results a detailed information about chemical species in dispersed Ca in this coal is not known. However, the main species in the SS070 raw coal is presumably similar to that in SS012 coal, namely "organically associated Ca" and "Ca particles of a size <1 μm". Some of these species would be transformed to CaS as above upon pyrolysis. However, since the atomic ratio of S/Ca in this coal is as low as 0.16, the formation of CaS is limited. Unreacted species remains as "Ca particles of a size <1 μm". The behavior of CCSEM-detectable Ca species during pyrolysis is quite different between the two coals, but for both the coals interaction of the dispersed Ca species as well as Ca-containing minerals with other minerals was not significant.

4.3. Fate of Ca during gasification

Interaction of Ca species with other ash particles commenced in the gasification stage. After the gasification, "Ca" (presumably CaO) still remained in the SS012 gasified char (Fig. 9a) and many particles were found in the Ca rich apex of the gasified char (Fig. 8b). It can be said that "Ca" in SS012 coal did not interact with other ash particles. In the case of SS070 coal, little "Ca" remained in the gasified char (Fig. 9b) and no particle was found in the Ca rich apex of the gasified char (Fig. 8d), indicating that "Ca" minerals interacted with other ash particles. The difference of reactivity of "Ca" minerals between the two coals may be a result of different mode of occurrence, but further investigation is needed to clarify the reason.

Dispersed Ca species drastically decreased during the gasification in both coals (Fig. 9). In the SS012 gasified char, particles with compositions ranging from the Ca rich apex towards the midpoint of the Si–Al join (Fig. 8b) were significant in comparison with the pyrolyzed char (Fig. 8a). This result suggests that the dispersed Ca is easy to interact mainly with kaolinite (Si/Al $\approx$ 1). In the case of SS070 gasified char, many particles around the Ca–Al–Si center were found in the gasified char (Fig. 8d), and these were not present in the pyrolyzed char (Fig. 8c). Since little particle was found on the Ca apex in the pyrolyzed SS070 char (Fig. 8c), the Ca–Al–Si particles in the gasified char might be formed as a result of the interaction of CCSEM-unquantifiable Ca with clay minerals. CCSEM-unquantifiable species including submicron CaS particles were converted into CCSEM-quantifiable species either by growing up by themselves and/or interacting with other ash particles to form "Ca–Al–Si" and "Ca–Fe–Al–Si" (Fig. 6). As shown in Fig. 6, pyrite decomposed during the pyrolysis to form "Fe". Then "Fe" was drastically reduced during gasification and transformed to "Ca–Fe–Al–Si" and "Fe–Al–Si". Zygarlicke et al. observed that in the initial stage of the combustion of Texas lignite, organically associated Ca was converted into Ca rich droplets, which often contained Fe–Al–Si [25]. In other words, the organically associated Ca cation and organically bound Fe and/or pyrite were incorporated into kaolinite-derived materials to form Ca–Fe rich aluminosilicate. Although the reaction conditions of the present study are different from those of Zygarlicke et al., the "Ca–Fe–Al–Si" fraction might be formed via a similar mechanism as in combustion.

4.4. Formation of low-melting point ash

Kaolinite ("Si–Al"), which is one of the dominant minerals in raw coal (Fig. 6), decomposes into amorphous quartz (SiO_2) and mullite ($3Al_2O_3 \cdot 2SiO_2$) during heating at around 900 °C [27]. Melting points of amorphous quartz and mullite are 1723 °C and 1850 °C, respectively. On the other hand, anorthite ($CaO \cdot Al_2O_3 \cdot 2SiO_2$) and gehlenite ($2CaO \cdot Al_2O_3 \cdot SiO_2$), which are most abundant ashes in the gasified char, have much lower melting points, 1550 °C and 1593 °C, respectively. Adhesion of "Si–Al" particles may not take place at around 1500 °C if they do not meet Ca species. However, if they interact with Ca-con-

taining species in the char matrix, they would be converted into ''Ca–Al–Si'' and ''Ca–Fe–Al–Si'' as is seen in Fig. 6. Therefore, such interaction leads to the lowering of melting point of ash as is well known. Generally this lowering is beneficial in entrain bed gasification but troublesome in fluidized bed gasification.

Na and K species can also form low-melting point ash by interacting with clay minerals. However, as described in Section 4.1, Na and K easily vaporized during gasification. Thus aluminosilicates in the char matrix would more readily interact with the dispersed Ca species that remains in the char during gasification. The formation of Ca-containing aluminosilicates predominantly contributes to the lowering of the melting point of ash during the gasification of the low rank coal.

5. Conclusions

Transformation of alkali and alkaline earth metals in sub-bituminous coals during CO_2 gasification were examined by combining ICP-AES and CCSEM techniques. The AAEM species in the sub-bituminous coals used in the present study were mostly present as dispersed species. Release of the AAEM species from the coal matrix during pyrolysis and the subsequent gasification was dependent on the type of metals. Na and K vaporized during the gasification and the interaction with inherent minerals was insignificant. Almost all the Ca and Mg retained in the gasified char even if major part of the carbon disappeared due to the gasification. Ca was the most abundant element among the AAEM and it significantly contributes to the formation of low-melting point ash. The dispersed Ca species were converted into submicron particles upon pyrolysis and then they interacted with clay minerals to form complex aluminosilicates of low-melting points.

Acknowledgement

This study was partially supported by NEDO under BRAIN-C program. The coal samples were provided from Japan Coal Energy Center (JCOAL).

References

[1] Sathe C, Pang Y, Li CZ. Energ Fuel 1999;13:748–55.
[2] Li CZ, Sathe C, Kershaw JR, Pang Y. Fuel 2000;79:427–38.
[3] Quyn DM, Wu H, Li CZ. Fuel 2002;81:143–9.
[4] Quyn DM, Wu H, Bhattacharya SP, Li CZ. Fuel 2002;81:151–8.
[5] Takarada T, Tamai Y, Tomita A. Fuel 1985;64:1438–42.
[6] Ohtsuka Y, Asami K. Catal Today 1997;39:111–25.
[7] Hengel TD, Walker Jr PL. Fuel 1984;63:1214–20.
[8] Chen Y, Shah N, Huggins FE, Huffman GP, Linak WP, Miller CA. Fuel Process Technol 2004;85:743–61.
[9] Zygarlicke CJ, Ramanathan M, Erickson TA. In: Proceedings of the engineering foundation conference on inorganic transformations and ash deposition during combustion, 1991. p. 525–44.
[10] Wilemski G, Srinivasachar S, Sarofim AF. In: Proceedings of the engineering foundation conference on inorganic transformations and ash deposition during combustion, 1991. p. 545–64.
[11] Shah N, Huffman GP, Huggins FE, Shah A. In: Proceedings of the engineering foundation conference on inorganic transformations and ash deposition during combustion, 1991. p. 179–90.
[12] Shah AD, Huffman GP, Huggins FE, Shah N, Helble JJ. Fuel Process Technol 1995;44:105–20.
[13] Miller SF, Schobert HH. Energ Fuel 1994;8:1197–207.
[14] Miller SF, Schobert HH. Energ Fuel 1994;8:1208–16.
[15] Helble JJ, Srinivasachar S, Boni AA, Kang SG, Graham KA, Sarofim AF, Beer JM, Gallagher NB, Bool LE, Peterson TW, Wendt JOL, Shah N, Huggins FE, Huffman GP. In: Proceedings of the engineering foundation conference on inorganic transformations and ash deposition during combustion, 1991. p. 209–28.
[16] Noda R, Takano T, Naruse I, Ohtake K. Kagaku Kogaku Ronbun 1997;23:635–43.
[17] Matsuoka K, Tomita A, Huggins F, Huffman G. Energ Fuel 2001;15:648–52.
[18] Matsuoka K, Suzuki Y, Eylands K, Benson SA, Tomita A. Fuel 2006;85:2371–6.
[19] Yamashita T, Akimoto A. In: Proceedings of 12th international conference on coal science and technology, 2005. 3D05.
[20] Morgan ME, Jenkins RG, Walker Jr PL. Fuel 1981;60:189–93.
[21] Benson SA, Holm PL. Ind Eng Chem Prod Res Dev 1985;24:145–9.
[22] Matsuoka K, Erlan R, Tomita A. Fuel 2002;81:1433–8.
[23] Matsuoka K, Takaya A, Tomita A. In: Proceedings of 21st annual international Pittsburgh coal conference, 2004. p. 32–4.
[24] Manzoori AR, Agarwal PK. Fuel 1992;71:513–22.
[25] Zygarlicke CJ, Steadman EN, Benson SA. Energ Combust Sci 1990;16:195–204.
[26] Punjak WA, Shadman F. Energ Fuel 1988;2:702–8.
[27] Couch G. Understanding of slagging and fouling in PF combustion. IEA Coal Res 1994.
[28] Guardani R, Drahos J, Giulietti M, Shugerl K. Fert Res 1989;20:181–91.
[29] Iwabu H, Koide N, Somiya I. Gesuidokyokaishi 1999;36:112–22.